Cao, W-J., Liu, W-S., Koh, C.G. and Smith, I.F.C. "Optimizing the operating profit of young highways using updated bridge structural capacity" Civil Structural Health Montoring, 10 (2) 2020, pp 219-234. This is a post-peer-review, pre-copyedit version of an article published in the Journal of Civil Structural Health Monitoring The final authenticated version is available online at:https://doi.org/10.1007/s13349-020-00379-3

Optimizing the operating profit of young highways using updated bridge structural capacity

Wen-Jun Cao[a,b]*, Wang-Sheng Liu[c], C. G. Koh[a] and I.F.C. Smith[b,d]

[a] Department of Civil and Environmental Engineering, National University of Singapore, Singapore

[b] ETH Zurich, Future Cities Laboratory, Singapore-ETH Centre, Singapore

[c] School of Civil & Environmental Engineering, Nanyang Technological University, Singapore

[d] Applied Computing and Mechanics Laboratory (IMAC), School of Architecture, Civil and Environmental Engineering (ENAC), Swiss Federal Institute of Technology (EPFL), Lausanne, Switzerland

Email: caowenjun@u.nus.edu/ wenjun.cao@arch.ethz.ch

Abstract

As more private firms participate in public projects aiming to increase their profits by adjusting operational strategies, there has been an increasing demand for structural identification in the operational phase. In this paper, we propose a framework for finding the optimal profit of toll highways over a five-year part of the operating period. Toll rates are adjusted using the updated safety condition of highway bridges as a constraint on the optimization task. The safety constraint explicitly reflects the requirement on the traffic volume based on the reserve capacity of bridges. The framework includes the following three steps. First, structural identification is carried out to identify parameter values of the bridge involved in the highway project. Then the reserve capacity under the relevant limit state is calculated based on the requirements of bridge design codes. The last step is to investigate the effects of reserve capacity on

the optimal operating profit. This framework is applied to a highway flyover project in Singapore. The optimal operating profit based on quantified reserve capacity increases compared to the case without information about reserve capacity. Also, the finding shows that the optimal profit will increase with the increases in values for the reserve capacity until the safety constraint is no longer critical.

Keywords:

Build-operate-transfer, model updating, multidisciplinary optimization, structural capacity, toll roads, static and dynamic testing

1. Introduction

from the public sector to construct, own, and operate the civil infrastructure that is stated in the concession contract. After a period of time, the firm transfers ownership to the government [1], [2]. Since this scheme allows the government to provide public facilities without using public funds, this type of project financing is popular around the world. According to the China Public-Private Partnerships Center under the Ministry of Finance, 13,554 PPP projects were registered nationwide with a total investment of $ 2.3 trillion by the end of June 2017 [3] (all values in this paper are in US dollars).

While the primary objective of a project owned by a government agency is to maximize the benefits for users, for example, congestion control [4], [5] and environment improvement [6], [7]), a private operator aims to increase its economic gains as much as possible within the contractual requirements [8]. In the context of highways and bridges, the profit-maximizing challenge has been formulated as a pricing optimization task in previous works [9], [10]. For instance, He et al. [11]

minimized the travel time and maximized the toll revenue of highways simultaneously by adjusting the toll rates.

Highway bridges are essential yet costly elements of highway networks. Related research has been focused on their safety condition including damage detection [12], upgrading assessment [13] and cost-optimized intervention planning (e.g. maintenance, repair, rehabilitation and replacement) [14].

The reserve capacity of highway bridges usually exceeds the safety level required in the design phase. Behaviour models are inherently safe due to high risks and construction-stage uncertainties [15]. The amount of reserve capacity following construction is unknown. To quantify it, the real condition of highway bridges in operation needs to be adequately assessed.

Structural identification (SI) methodologies have the potential to provide accurate assessments of the current condition of structures, including highway bridges, through updating behavior models using measurements. For highway bridges, measurements such as displacements, strains, mode shapes and natural frequencies are acquired by static and dynamic testing. A significant amount of research has focused on SI; see [16] and [17] for comprehensive literature reviews. Traditional SI methodologies, such as residual minimization, involve determining a set of model-parameter values that minimizes the discrepancy between model predictions and measurements [18], [19]. Under the assumption of deterministic model-parameter values, the accuracy of the solutions to this form of optimization is dependent upon the presence of uncertainties, particularly systematic model uncertainties, arising from sources such as model fidelity, boundary conditions, geometric discrepancy and safe design assumptions.

An alternative way to perform structural identification is through Bayesian model updating [20]–[22]. In this methodology, both model parameters and errors involved in prediction are considered to be random variables, thereby providing a rational framework for dealing with uncertainties. However, the accuracy of Bayesian model updating can be influenced by the forms of uncertainty distribution, bias and correlations. With incomplete knowledge, the identified parameter values may be unsafe. [15], [23]

Recently, Goulet and Smith [23] proposed a new method called error-domain model falsification (EDMF) for situations where the dependencies between uncertainty sources are not available. In this method, a set of plausible model instances defined by parameter-value combinations are generated and their predictions are calculated. A model instance is falsified if the difference between its predictions and measurements lies outside of the region derived from combining modeling and measurement errors. More recently, Pai et al. [24] showed that EDMF is compatible with a modified formulation of Bayesian model updating. However, EDMF satisfies engineering requirements better than standard Bayesian approaches [24].

In this paper, we propose a framework for maximizing the operating profit of toll highways over a five-year period by adjusting the toll rates and taking the updated safety condition of bridges into account. Specifically, given structural information from measured data, EDMF is used to obtain the updated model instances that predict the current reserve capacity of the bridge under study. Safety constraint is imposed as the effects of traffic loading should not exceed the predicted reserve capacities. The influence of introducing the safety constraint is investigated using an example involving a highway bridge in Singapore. Using this example, the effect of the magnitude of the

reserve capacity on the optimal profit is studied. Since the focus of this study is on young bridges, major damage and maintenance costs are not included.

The rest of this paper is organized as follows. First, the background of EDMF and the formulation of the profit-maximizing goal are presented in Section 2 and Section 3 respectively. The formulation includes the safety constraint along with other constraints. Section 4 further discusses the safety constraint in detail. An example is studied in Section 5 to illustrate the implementation of this framework and to investigate the influence of updating the bridge condition. Finally, the discussion of the results and conclusions are presented in Section 6 and Section 7 respectively.

2. Background to the EDMF method

The central idea of EDMF is to falsify the model instances from a pool of plausible models (instances of a model class) based on the discrepancy between predictions and measurements. When uniform probability distributions are employed, the thresholds of falsification can be determined without the consideration of error dependence between sensor measurements.

Consider a model class $g(\boldsymbol{\theta})$ that predicts a quantity of interest y (structural responses such as deflection and strain for bridges), which involves a vector of n parameters $\boldsymbol{\theta} = [\theta_1, \theta_2, \dots, \theta_n]$. If the true values of parameters $\boldsymbol{\theta}^*$ are known a priori, the sum of the prediction of this model $g(\boldsymbol{\theta}^*)$ and the modeling error ϵ_{model} equals to the true output y_{true}. Meanwhile, y_{true} can be obtained as the sum of the corresponding measurement y_{meas} and measurement error ϵ_{meas}. Therefore, given the additive errors, the relationship between the prediction and measurement can be written as

$$g(\boldsymbol{\theta}^*) + \epsilon_{model} = y_{true} = y_{meas} + \epsilon_{meas} \tag{1a}$$

$$g(\boldsymbol{\theta}^*) - y_{meas} = U_c \tag{1b}$$

Due to the unavailability of y_{true} and random nature of errors, the combined error is treated as a random variable U_c described by a probability density function $f_{U_c}(\epsilon)$. A model instance (i.e., a realization of $\boldsymbol{\theta}$) will be falsified if the discrepancy between its prediction and the corresponding measurement (the observed residual in the left-hand side of Equation (1b)) is not within the threshold bounds derived from U_c at measurement locations. **Fig. 1** shows the threshold bounds $[T_{min}, T_{max}]$ for a univariate normal distributed error where T_{min} and T_{max} are the lower and upper bounds respectively. Similar to the concept of confidence interval, the threshold bounds represent the narrowest interval in which the integral of $f_{U_c}(\epsilon)$ is ϕ, meaning that the probability of wrongly discarding correct models is $1 - \phi$.

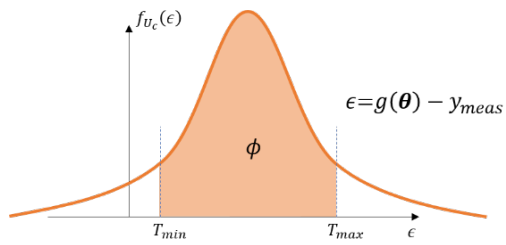

Fig. 1: Threshold bounds in EDMF for the combined error $\boldsymbol{U_c}$

For multiple measurements, a model instance will be falsified when any of its observed residuals $g_i(\boldsymbol{\theta}) - y_{meas,i}$ ($i \in [1,2,\cdots,m]$), where m represents the number of measurements, lies outside the corresponding threshold bounds $[T_{min,i}, T_{max,i}]$. The threshold bounds mark the narrowest interval in which the integral of $f_{U_{c,i}}(\epsilon)$ is $\phi^{1/m}$. The thresholds bounds can be given by

$$T_{min,i} = F_{U_{c,i}}^{-1}\left(\frac{1}{2}\left(1-\phi^{1/m}\right)\right) \tag{2a}$$

$$T_{max,i} = F_{U_{c,i}}^{-1}\left(1-\frac{1}{2}\left(1-\phi^{1/m}\right)\right) \tag{2b}$$

where $F_{U_{c,i}}^{-1}(\cdot)$ is the inverse cumulative distribution function of $U_{c,i}$. The expression $\phi^{1/m}$ is used (rather than ϕ) to ensure constant probabilities for varying numbers of measurement locations. As m increases, $\phi^{1/m}$ tends to 1.

In EDMF, detailed finite element models are built based on engineering information (including design drawings and/or on-site inspection). Modeling and measurement uncertainties are quantified using sensor specifications, modeling knowledge of finite element method and engineering judgment. If all initial model instances are falsified, the model class is rejected. This often originates from wrong assumptions in the model class or uncertainty levels. Site inspection and new measurements can be used to improve the model class. For details, readers can refer to the framework proposed in [25].

The model falsification procedure is conservative in the sense that the probability of wrongly discarding the correct model is no more than $1-\phi$. After model updating, the updated model is described by a set of remaining model instances $\{\boldsymbol{\theta}\}_u$ (i.e., candidate models (CMS)), which can predict more accurately the future performance of the system under study.

3. Formulation of profit optimization

Consider a highway link consisting of one or more bridges. It is commonly the case that toll rates are charged for a range of vehicle types. Also, the toll rates for multi-type

vehicles affect the traffic composition greatly, which further influences the traffic load acting on the bridges. In this paper, for a set of vehicle types $\mathcal{K}$ traveling on the highway, a unique toll rate x_k is charged for each vehicle type $k \in \mathcal{K}$. The toll rates can be denoted by $\boldsymbol{x} = [x_k]_{k\in\mathcal{K}} \in \mathbb{R}^{|\mathcal{K}|}$ where $|\mathcal{K}|$ is the cardinality of set $\mathcal{K}$.

Assume that at year t_0 the condition of the bridges in the highway link is assessed by conducting static and/or dynamic tests. The objective is to maximize the operating profits in the following Δt years (typically $\Delta t \geq 1$, a Δt of five years is assumed in this study) by adjusting toll rates $\boldsymbol{x}$. It is assumed that it is a young bridge that needs no major maintenance interventions. For the fixed capacity y of an existing highway, the traffic volumes $\boldsymbol{v} = [v_k]_{k\in\mathcal{K}} \in \mathbb{R}^{|\mathcal{K}|}$ corresponding to the toll rates $\boldsymbol{x}$ can be estimated based on the supply-demand equilibrium condition [26]. Both the toll rates $\boldsymbol{x}$ and traffic volumes $\boldsymbol{v}$ are restricted to make sure that $\boldsymbol{x}$ is within the box bound $\boldsymbol{x}_{min} \leq \boldsymbol{x} \leq \boldsymbol{x}_{max}$ and the load does not exceed the capacity of the highway. Furthermore, bridges in service may experience varying traffic loads depending on the site-specific traffic volumes and the characteristics of heavy vehicles. After the bridge condition assessment, the reserve capacity of the bridges is calculated to provide an upper bound for the anticipated traffic loads. This optimization challenge is formulated as

$$\begin{aligned} \max_{\boldsymbol{x}} \quad & P(\boldsymbol{x}) = \sum_{t=t_0}^{t_0+\Delta t} \left[\sum_{k\in\mathcal{K}} x_k \cdot v_k(x_k) - M\delta_M(t) - H\delta_H(t) - OP \right] - CC \\ s.t. \quad & (a) \quad \boldsymbol{x}_{min} \leq \boldsymbol{x} \leq \boldsymbol{x}_{max}, \boldsymbol{x} \in \mathbb{R}^{|\mathcal{K}|} \\ & (b) \quad \sum_{k\in\mathcal{K}} v_k \cdot \alpha_k \leq y \\ & (c) \quad W(\boldsymbol{v}) \leq RCap \end{aligned} \tag{3}$$

In Equation (3), $P(\boldsymbol{x})$ represents the total operating profit in the period Δt given a specific toll rate scheme. It is assumed that the traffic flow is in a stationary state, i.e.,

the traffic volumes $\boldsymbol{v}$ remain unchanged between two condition assessments at t_0 and $t_0 + \Delta t$. The routine maintenance costs and minor rehabilitation cost are denoted by M and H, respectively. $\delta_M(t)$ and $\delta_H(t)$ are indicator functions which are equal to one if maintenance or rehabilitation is conducted at time t_0, otherwise they are zero. OP is the operating cost during the time period studied. In the objective function, the last term CC is the cost of the condition assessment, which is conducted only at time t_0. Three constraints of interest are summarized in Equation (3): (a) box bounds of $\boldsymbol{x}$; (b) the designed traffic volume should not exceed the highway capacity y which is determined by the number of lanes in practice. The designed traffic volume is calculated by multiplying the equivalent passenger car units (PCU) of vehicle type k (denote as α_k) and the traffic volume of vehicle type k; and (c) safety constraint based on the updated condition of bridges. Constraint (c) will be discussed in detail in Section 4.

For vehicle type k, its toll revenue $x_k \cdot v_k(x_k)$ per time unit relies on the interaction of the traffic supply and demand. The demand for highway transportation represents the users' willingness to pay for a trip. If the toll rate falls, the quantity of the demand will increase. The toll-dependent traffic demand is expressed as

$$v_k = D(\boldsymbol{\xi}_k, u_k) \tag{4}$$

where $D(\cdot)$ denotes the demand function, which is given in terms of its parameters $\boldsymbol{\xi}_k$ and the total travel cost of a trip u_k. For highway users, the total travel cost u_k includes two parts, i.e., the user time cost $\beta_k t_k(v_k)$ and the toll rate x_k:

$$u_k = \beta_k t_k(v_k) + x_k \tag{5}$$

where $t_k(\cdot)$ is the travel time function and β_k is the users' value of time which converts the travel time into the monetary cost. Thus, let $B(\cdot)$ be the inverse function of $D(\cdot)$ or

the benefit function, and the traffic demand v_k can be derived based on the supply-demand equilibrium:

$$x_k(v_k) = B(v_k, \boldsymbol{\xi}_k) - \beta_k t_k(v_k) \tag{6}$$

One of the most widely used link travel time estimator is the Bureau of Public Roads (BPR) function [27]. It is proposed by the United States Federal Highway Administration as follows:

$$t(v) = t^0[1 + r_1(v/y)^{r_2}] \tag{7}$$

where $t^0$is the free-flow travel time on the link; r_1 and r_2 are the first and second BPR function parameters, respectively (classically $r_1 = 0.15$ and $r_2 = 4.0$ [27]).

However, the standard BPR function does not account for heterogeneity in traffic flows. Lu et al. [28] developed the microscopic traffic simulation based four-step method to estimate the travel time functions of heterogeneous traffic flows on a freeway. They considered three vehicle types: passenger car, light trucks, and heavy trucks. The piecewise travel time functions for the three vehicle types are summarized as follows:

For cars (k = 1),

$$t_1 = \begin{cases} t_1^0\left[1 + 0.29(1+\rho_3)^{1.52}(1+\rho_2)^{1.98}\left(\sum_{k\in\mathcal{K}} v_k \cdot \alpha_k/y\right)^{1.55}\right], & \rho_1 \geq 55\% \\ t_1^0\left[1 + 0.57\left(\sum_{k\in\mathcal{K}} v_k \cdot \alpha_k/y\right)^{1.12}\right], & \rho_1 < 55\% \end{cases} \tag{8}$$

For light trucks (k = 2),

$$t_2 = \begin{cases} t_2^0\left[1 + 0.08(1+\rho_3)^{1.17}(1+\rho_2)^{0.57}\left(\sum_{k\in\mathcal{K}} v_k \cdot \alpha_k / y\right)^{2.07}\right], & \rho_1 \geq 55\% \\ t_2^0\left[1 + 0.10\left(\sum_{k\in\mathcal{K}} v_k \cdot \alpha_k / y\right)^{1.84}\right], & \rho_1 < 55\% \end{cases} \tag{9}$$

For heavy trucks ($k = 3$),

$$t_3 = \begin{cases} t_3^0\left[1 + 0.12\left(\sum_{k\in\mathcal{K}} v_k \cdot \alpha_k / y\right)^{1.98}\right], & \rho_1 \geq 55\% \\ t_3^0\left[1 + 0.106\left(\sum_{k\in\mathcal{K}} v_k \cdot \alpha_k / y\right)^{1.78}\right], & \rho_1 < 55\% \end{cases} \tag{10}$$

where ρ_i is the proportion of vehicle type i.

The benefit function $B(\cdot)$ is commonly assumed to be a continuously decreasing and differentiable function with a vector of deterministic parameters $\boldsymbol{\xi}_{\mathrm{k}}$. In this paper, three forms of $B(\cdot)$, i.e., negative exponential, linear and polynomial, will be studied in the example in Section 5.

It can be observed that Formulation (3) is a constrained nonlinear optimization task, the objective of which is to set the optimal toll rate $\boldsymbol{x}$ (thereby controlling the traffic volume) to maximize the operating profit through the period Δt. Since the toll rate x_k is given explicitly in terms of v_k as indicated in Equation (6), it is more convenient to set $\boldsymbol{v}$ as the design variable and rewrite Formulation (3) as

$$\begin{aligned} \max_{\boldsymbol{v}} \quad & P(\boldsymbol{v}) = \\ & \sum_{t=t_0}^{t_0+\Delta t}\left[\sum_{k\in\mathcal{K}} v_k \cdot \left(B(v_k) - \beta_k t_k(v_k)\right) - M\delta_M(t) - H\delta_H(t) - OP\right] - CC \\ s.t. \quad & (a) \quad \boldsymbol{x}_{min} \leq B(v_k) - \beta_k t_k(v_k) \leq \boldsymbol{x}_{max}, B(v_k) - \beta_k t_k(v_k) \in \mathbb{R}^{|\mathcal{K}|} \\ & (b) \quad \sum_{k\in\mathcal{K}} v_k \cdot \alpha_k \leq y \\ & (c) \quad W(\boldsymbol{v}) \leq RCap \end{aligned} \tag{11}$$

4. Structural safety constraint with the updated bridge condition

In the optimization scheme, the structural safety condition is introduced as constraint (c) in Formulation (11). The right-hand side of constraint (c) is the reserve capacity $RCap$ calculated based on the updated structural condition, providing the upper bound for the traffic loads in the safety constraint. The reserve capacity is defined as the ratio of the traffic loads the bridge can take to the ones specified by the Eurocode. The actual load factor $W(\boldsymbol{v})$ is defined as the ratio of the maximum loads that a bridge will encounter based on historical traffic records to the design loading.

4.1 Reserve capacity

Based on the updated model of a highway bridge, its current safety condition is measured in terms of reserve capacity in this paper. Reserve capacity (beyond the reserve provided by safety factors) exists in most civil infrastructure, as discussed in [29]–[32].

During the engineering design of structures, the fundamental requirements are to sustain all actions that are likely to occur and to remain fit for the required use for a certain level of reliability during their intended life. Structures should satisfy two principal criteria: the ultimate limit state (ULS) and the serviceability limit state (SLS). While ULS describes situations (including fatigue) that may lead to the collapse of the structure, SLS is concerned with its functioning, comfort and appearance. Consider a limit state function $h(\boldsymbol{\theta})$:

$$h(\boldsymbol{\theta}) = R - S \tag{12}$$

where R represents the capacity or resistance of a structure and S represents the effect of actions. For a limit state, the failure event of the structure occurs when $h(\boldsymbol{\theta}) < 0$. In

order to sustain the structural reliability, the failure probability $P_F(\boldsymbol{\theta})$ defined as follows:

$$P_F(\boldsymbol{\theta}) = Prob(h(\boldsymbol{\theta}) < 0) \tag{13}$$

should not exceed the target failure probability $[P_F]$. The allowable failure probability maps to the target reliability index [33], which may differ amongst different limit states.

The reserve capacity for SLS is determined in an iterative way as shown in **Fig. 2**. First, the design loads are applied to each candidate model to compute the effect of loads $S(\boldsymbol{\theta})$ (such as deflection or stress for bridges). Then the CMS failure probability P_F is computed by adding the modelling uncertainty to the CMS prediction. If the failure probability is smaller than $[P_F]$, a load factor $LF > 1$ is iteratively applied to the traffic loads, as described in Section 5.3. The iteration continues until the estimated P_F equals $[P_F]$ and the value of the load factor at the final iteration is denoted as LF_{SLS}. Finally, the SLS reserve capacity is estimated as $RCap_{SLS} = LF_{SLS}$.

For ULS, the reserve capacity is quantified using the global resistance safety factor [34]. The flowchart is shown in **Fig. 3**. The factor γ_R accounts for the uncertainty caused by geometry, modelling and material variations. The random variation of material properties is estimated using two non-linear simulations: the first adopting mean values of material properties $U_1(\boldsymbol{\theta_m})$, the second including characteristic values of material properties $U_1(\boldsymbol{\theta_k})$. All vertical loads are increased by means of two load factors LF_m, LF_k until failure is reached. This procedure (depicted in **Fig. 3**) allows the computation of the global safety factor γ_R. Meanwhile, the model class including mean values of material properties $U_2(\boldsymbol{\theta_m})$ is used to determine the load factor LF_{ULS} which is applied to the traffic loads in order to reach structural failure. The ULS reserve capacity $RCap_{ULS}$ is then calculated as the ratio between LF_{ULS} and γ_R. More details

are provided in Section 5.3.2. The overall reserve capacity for this bridge is taken as $RCap = min\,\{RCap_{SLS}, RCap_{ULS}\}$.

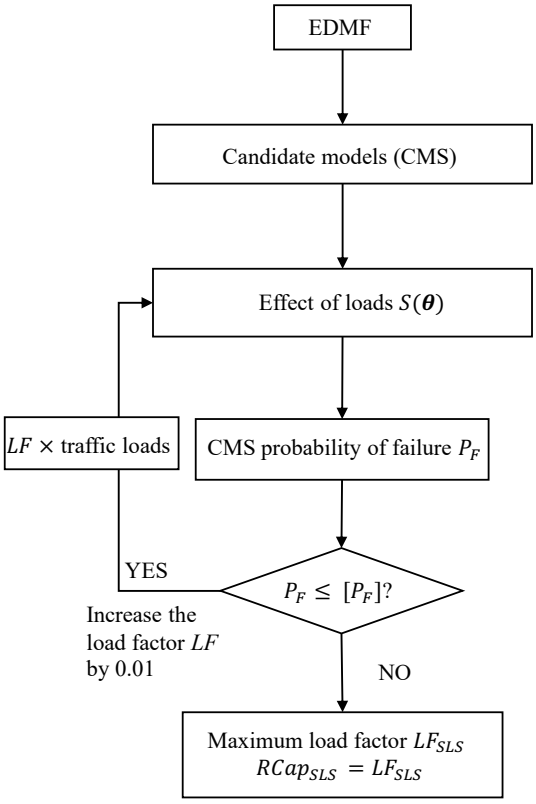

Fig. 2: Flowchart to determine the reserve capacity for serviceability limit state, from [32]

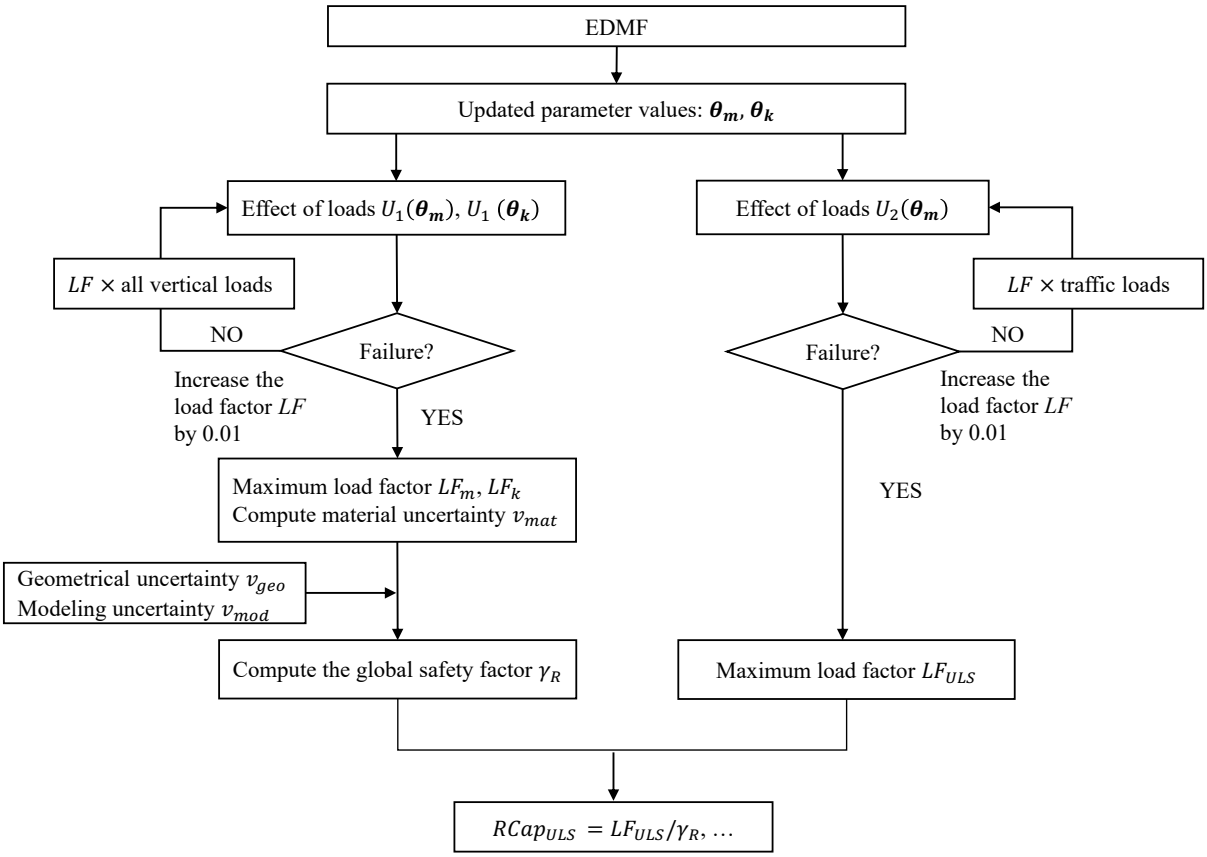

Fig. 3: Flowchart to determine the reserve capacity for ultimate limit state, adapted from [32]

4.2 Traffic loads on bridges

For an existing highway bridge, the load factor W is usually determined by the extreme loads that the bridge will experience in the traffic environment during its remaining service life. Traffic loads are related to factors such as gross vehicle weights, vehicle class (usually defined by the number of axles), and axle configurations for the heavy vehicles. In practice, traffic loading maybe estimated from measured traffic data.

From a probabilistic viewpoint, if there is, for example, either an above-average traffic volume or the area has a high proportion of heavy vehicles, then there is a greater probability that the maximum loading increases, and the design loading is exceeded. When there is a low traffic volume or heavy vehicle proportion, the probability that the

design loading is exceeded is lower than for average traffic volume or average heavy vehicle proportion [35].

The factors influencing the value of W vary with specific sites, traffic environment and bridge types. Leahy et al. [36] investigated the effects of traffic growth (traffic volume and vehicle weight) on characteristic bridge load and they inferred that the growth significantly affected the load effects. Specifically, 1% annual growth in flow caused an average 6% increase in load effects and 1% annual growth in truck weight caused an 43% increase in load effects.

OBrien et al. [37] investigated the effects of four traffic volume growth (1%, 2%, 3%, and 4.1% annual growth) on bridges with varies lengths (15m, 20m, 25m, and 30m). The authors inferred that the growth of traffic volume generates an increase in characteristic maximum load effects and the load effects increase with the growth rates.

Furthermore, similar findings regarding the growth of the traffic volume and the truck weight are obtained in [38]. Besides, Yu et al. [38] also considered the effects of the growth of the proportion of heavy trucks. It is found that the proportion of heavy trucks have similar effects on the growth of traffic volume on the predicted load effects. The growth of the proportion of heavy trucks leads to an increase of 3% to 25% in the maximum lifetime traffic load effects.

Kim et al. [35] analyzed the annual extreme load effect according to various traffic environment for both pre-stressed concrete and steel box girder bridges in Korea. The results showed that for the environments and bridge types that were studied, the annual extreme loading tends to increase in proportion to the average daily traffic volume and heavy vehicle proportion.

Overall, the growth of the traffic volume, the proportion of heavy vehicles and the truck weight are considered as three key factors that influence the value of W.

Among them, the change of truck weight is unlikely to occur within a short term without significant changes in legislation for allowable weight limits. Thus only traffic volume and heavy-vehicle proportions are considered in this paper.

5. Case study

5.1 Description

In this section, a highway (in operation) in Singapore was investigated. This example was calibrated to be representative for toll highways that was built in the last 20 years. The operating time per day was assumed to be 12 hours instead of 24 hours to guarantee that the total revenue in this case study was more realistic. This is because in the case study, we did not consider the change of toll rates with seasons and peak hours. Furthermore, the design traffic volume was usually larger than the real volume. The capacity of this highway was 2200 Passenger Car Unit (PCU) per hour.

The highway length was assumed to be 100 km with two lanes throughout and 15 bridges along this highway. Normally, highways tolls were charged per km. Since there was no bypass along this highway, the toll rate was presented as the total charge of 100 km. The condition assessment of bridges was carried out every five years (Δt =5) and it costed \$0.2M per assessment per bridge. The operating cost was \$0.05M per km per year. It was assumed that the routine maintenance was carried out every year, and each time the cost was \$0.15M per km. The cost of pavement rehabilitation was assumed to be \$20M for this highway. In reality, the operating cost and maintenance cost may vary over years due to the variation in labor cost and the aging of structures. In this case study, we assumed that costs are fixed during 5 years.

For illustration purpose, it was assumed that among 15 bridges, Bridge A was taken to be the most critical bridge with respect to reserve capacity. Also, it was

assumed that if all reserve capacity was used, no other bridge became critical. The structural identification and reserve capacity of Bridge A have been investigated in detail in Section 5.2 and 5.3.

(a)

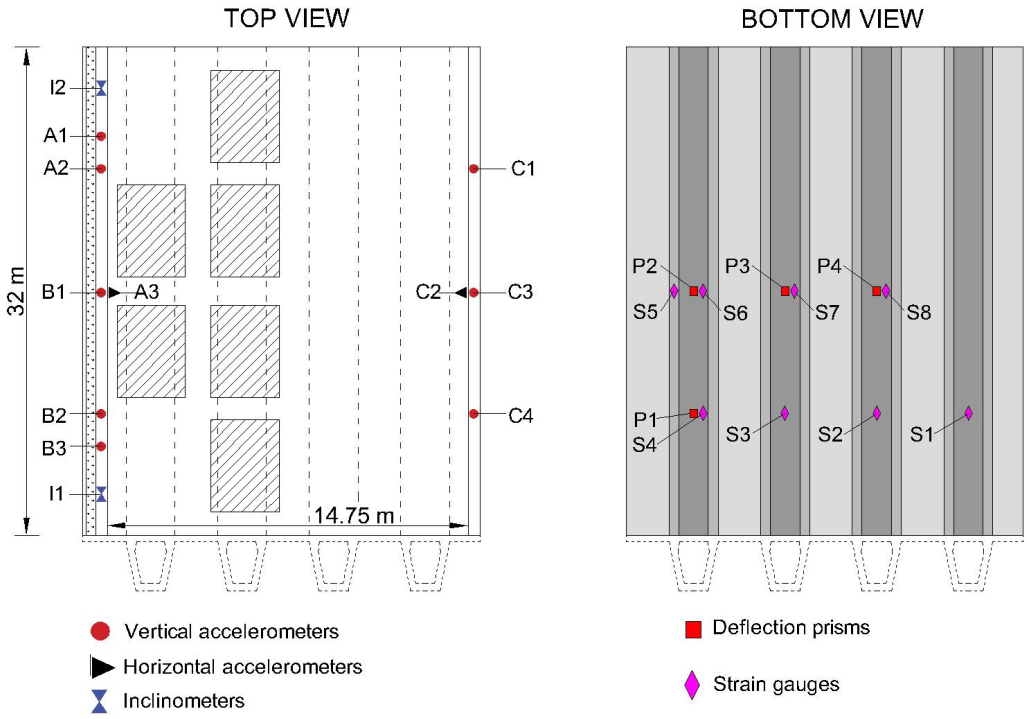

(b)

Fig. 4: (a): Photograph of the static test performed on Bridge A;

(b): Sensor configuration and truck configuration in the static test: top view and bottom view

Bridge A is a one-span pre-stressed reinforced concrete bridge of 32m length and 16m width (shown in **Fig. 4(a)**). The superstructure consists of four precast beams

and a concrete deck. Both static and dynamic tests have been carried out for structural identification.

In the static tests, six trucks of approximately 32t each were loaded on the bridge. Four deflections (P1~P4), two inclinations (I1~I2) and eight strains (S1~S8) were measured at fourteen locations. The configurations of trucks and sensors are shown in **Fig. 4(b).** In the dynamic tests, ten accelerometers (A1~A3, B1~B3, C1~C4) (shown in **Fig. 4(b)**) were installed along the bridge to capture the natural frequencies and mode shapes. Both free-vibration data and ambient vibration data were used to identify the modal properties of the bridge. According to modal analysis, two bending modes, one torsional mode and one lateral bending mode were obtained (shown in **Fig. 5**).

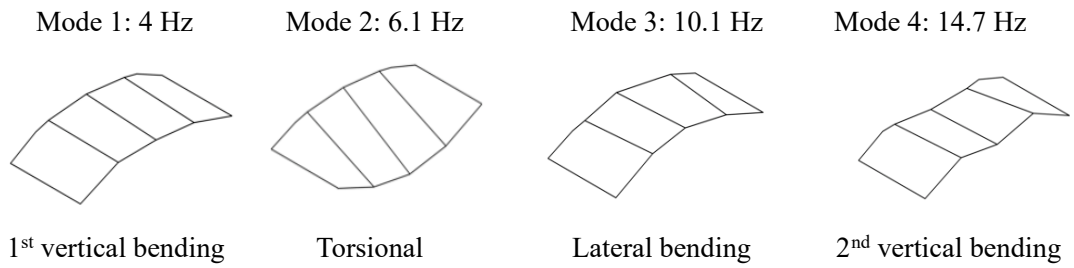

Fig. 5: The natural frequencies and mode shapes that are identified

As shown in **Fig. 4(b)**, all dynamic sensors were installed along the two sides of the bridge. Since there was no accelerometer at mid-span, the mode shape obtained for Mode 3 is similar to the mode shape for Mode 1. Using the knowledge of dynamic mechanical properties of the simply supported beam, Mode 3 is identified as a lateral bending mode.

5.2 Structural identification

Parameter values that are identified include the Young's modulus of concrete (E), the density of the bridge (D), the logarithm of the bending stiffness of bearings

(LogB) and the logarithm of the vertical stiffness of bearings (LogV). These parameters are defined based on the sensitivity analysis and their initial ranges are defined using engineering judgment [39]. Measurement and modeling uncertainties are fixed based on work by Cao et al. [39]. To obtain a sufficient size of model instances, surrogate models are fitted using Gaussian processes [40]. A total number of 50^4 = 6,250,000 samples are generated by grid sampling (50 discrete values for each parameter). Adopting the framework of system identification using both static and dynamic measurements, six abnormal strain measurements are removed from the measurement set [39]. **Fig. 6** shows the final results of the identification. A total number of 1,119 candidate model instances are obtained.

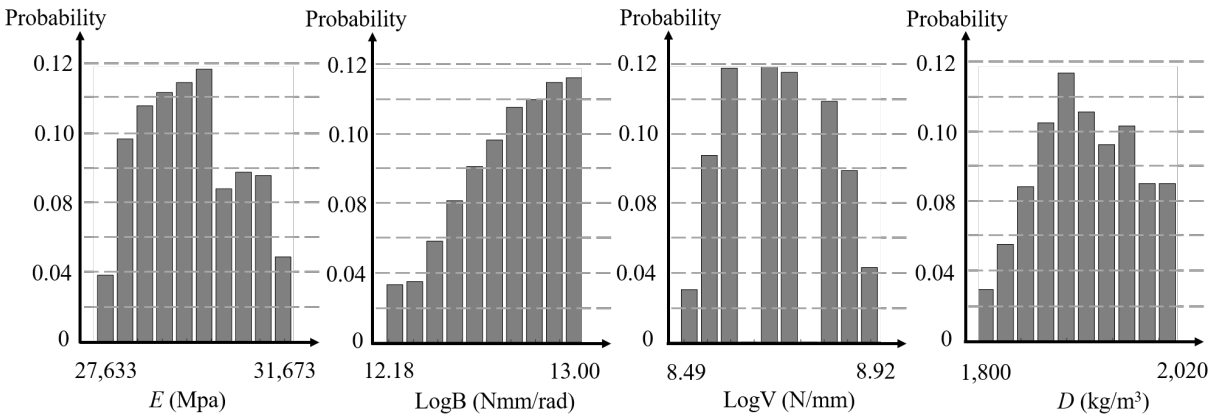

Fig. 6: Histogram of structural identification using EDMF

5.3 Estimation of reserve capacity

Truck traffic is categorized into two types of trucks: standard trucks and permit trucks. Permit trucks exceed the normal allowable weight and are calculated separately [41]. In Eurocode specifications of traffic load, Load Model 1 is used for standard trucks and Load Model 3 is used for permit trucks. Load Model 1 is intended to cover flowing, congested or traffic jam situations with a high proportion of heavy lorries. In this paper, Load Model 1 was investigated as the possibility of exploring operating profits was

investigated within the permit weight limit given in the Eurocode.

5.3.1 Serviceability limit state

For the serviceability limit state, crack control is found to be critical in this case study. As it is a prestressed bridge and according to its exposure class, crack control requires that no tensile stress occurs in the concrete around the bonded tendons. As a result, the serviceability limit state is defined as when the compressive normal stress of concrete reaches zero. Loads include permanent action, the prestressing force imposed on the bridge, traffic loads and these three are combined under the frequent load combination in Eurocode [42].

First, the predictions of candidate model instances are calculated with the traffic loads specified in the Singapore code using safety factor LF=1.0 for serviceability. In this paper, the modeling uncertainty sources of stress include model simplification and numerical errors in FE methods (e.g. mesh refinement), see **Table 1** and Proverbio et al. [32] for more information. In the second step, modeling uncertainties of stress are added into the CMS stress predictions using the Monte Carlo method [32]. The methods for adding modeling uncertainties to predictions vary with applications. For example, in the online force identification problem, Lai et al. [43] derived a new normalized standard deviation of the input identification error to interpret the accuracy of the sequential deconvolution input reconstruction method. Then, the load factor is increased in steps until the probability of failure P_F meets the standard value of failure probability for SLS ($[P_F] = 0.1$ for a 50-year period [33]). The increment step of LF is 0.01 which is set as 10% of $[P_F]$.

Table 1: Modelling uncertainty sources of stress

Uncertainty source	Stress	
	Min	Max
Model simplification and FE method (%)	-5	13
Mesh refinement	-1	1
Additional uncertainty	-1	1

Finally, the deflection and stresses are checked to see if they satisfy the requirements of the code. As shown in **Fig. 7**, when LF_{SLS}= 1.72, the failure probability P_F reaches the limit state condition $RCap_{SLS}$ =1.72.

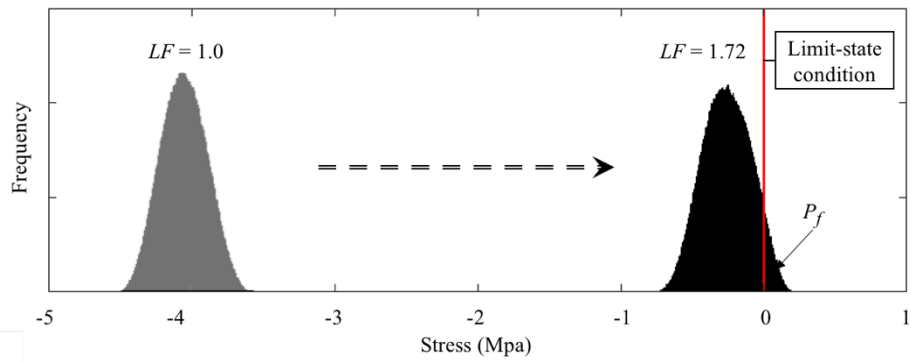

Fig. 7: CMS stress-prediction distribution (SLS)

5.3.2 Ultimate limit state

Statistical studies indicate that the probability distribution of resistance of reinforced concrete members can be described by a two-parameter lognormal distribution with the lower bound at the origin [34]. These two parameters are LF_m-mean resistance and v_R-coefficient of variation of resistance.

The global resistance factor γ_R is determined from

$$\gamma_R = exp\ (\alpha_R \cdot \beta \cdot v_R) \tag{14}$$

where α_R is a sensitivity (weighting) factor for the reliability of resistance, β is a reliability index and v_R is the combined coefficient of variation due to modeling, geometrical and material uncertainties, denoted as v_{mod}, v_{geo} and v_{mat}, respectively.

The estimation of v_R is a challenging task. Since it influences the value of reserve capacity significantly, cases under various assumptions are investigated. In Case I, only material uncertainty is considered. i.e. $v_R = v_{mat}$.

v_{mat} is determined from

$$v_{mat} = \frac{1}{1.65} \cdot \ln \left[\frac{LF_m}{LF_k}\right] \tag{15}$$

where LF_m/LF_k is the resistance value calculated using the mean/ characteristic values of material parameters [34]. These load factors are applied to the global vertical load of structure (i.e., the sum of permanent and variable loads) [33].

The design resistance is calculated from

$$RCap_{ULS} = \frac{LF_{ULS}}{\gamma_R} \tag{16}$$

where LF_{ULS} is applied only to traffic loads and is calculated using the mean values of material parameters.

In Case II, all three uncertainties are considered. v_{mat} is calculated from Equation (16). v_{mod} and v_{geo} are set to be 0.05, following the assumptions in [44]. These coefficients of variation are assumed as the basis for the partial factors given in EN 1992-1-1 (European Concrete Platform ASBL, 2008) [44]. The combined coefficient of variation v_R is calculated as suggested in [44].

$$v_R = \sqrt{v_{mat}^2 + v_{mod}^2 + v_{geo}^2} \tag{17}$$

In Case III, the ECOV (estimation coefficient of variation) approach is adopted. In calculating v_R, the effects of modeling and geometrical uncertainty are not considered. The modeling uncertainty is included in the calculation of design resistance:

$$RCap_{ULS} = \frac{LF_{ULS}}{\gamma_R \cdot \gamma_{Rd}} \tag{18}$$

where γ_{Rd} is the model uncertainty factor; for well validated numerical models it is proposed as γ_{Rd} =1.06.

When bridges approach their ultimate limit states, boundary conditions are no longer the same as the ones in the load tests. For example, no pin-support rigidity can be assumed. Young's modulus of concrete, which is identified in the elastic domain, contributes marginally to the ultimate limit state. Among all identified parameters, the density of the concrete affects the results by influencing the value for the dead load applied on the bridge. The density ranges are 1800 to 2020 kg/m^3.

A 2D nonlinear model is built using the software JCONC [45]. With the increase of the load, the tendons gradually yield (dark red areas) and the compressive stress in the concrete deck gradually reaches the maximum compressive stress (black mesh elements). The criteria are met when $LF_m = 1.38$, $LF_k = 1.30$, $LF_{ULS} = 1.66$ respectively.

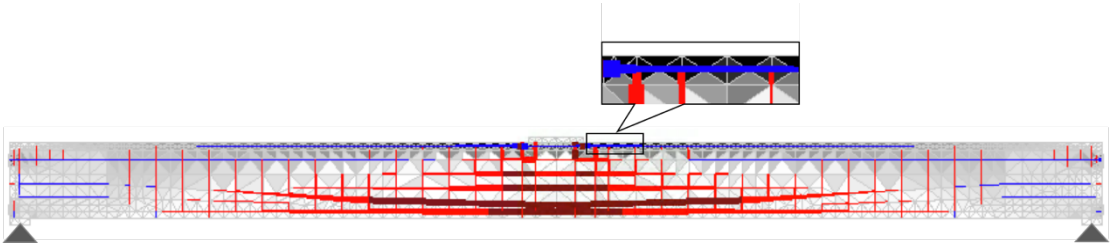

Fig. 8: 2D non-linear finite-element analysis when LF_{ULS} =1.66, performed using JCONC.

The results of the three cases are shown in **Table 2**. Case II gives the lowest value of reserve capacity while Case I provides the largest value which is 15% and 6% larger than the assessment in Case II and Case III, respectively.

Table 2: Comparison of $RCap_{ULS}$ using three assumptions

	Case I		**Case II**		**Case III**	
$\boldsymbol{v_{mat}}$	γ_R	$RCap_{ULS}$	γ_R	$RCap_{ULS}$	$\gamma_R \cdot \gamma_{Rd}$	$RCap_{ULS}$
0.036	1.116	1.49	1.273	1.30	1.183	1.40

5.4 Maximum operating profit

As mentioned in Section 4.2, W is assumed solely dependent on the traffic volume and the proportion of heavy vehicles [35]–[38]. For illustration, a linear relation is assumed:

$$W(\boldsymbol{v}) = c_1 \frac{\sum_{k \in \mathcal{K}} v_k \cdot \alpha_k}{y} + c_2 \rho_h + const \tag{19}$$

where c_1 and c_2 are coefficients that determine the weightings of traffic volume and heavy-vehicle proportion respectively; total traffic volume $\sum_{k \in \mathcal{K}} v_k \cdot \alpha_k$ (passenger car unit (PCU)) is normalized by the traffic capacity y (PCU) of the highway; ρ_h is the proportion of heavy vehicles in the traffic flow.

Situations where the extreme loading cannot be calculated in this manner are e.g., the local authority agrees to increase the allowable weight limit or new permissions

for special vehicles. In this study, it is assumed that such situations are not present and conditions where W depends on traffic volume and heavy-vehicle proportion prevail. In practical applications the accuracy of this relationship should be verified by traffic load data.

5.4.1 Scenario I: Homogeneous traffic

In this scenario, the vehicle traffic is assumed to be homogeneous without distinguishing trucks from cars. The classic BRT function (Equation (7)) is adopted to estimate the travel time. Three typical benefit functions (shown in **Table 3**) [46] are compared. The corresponding relations of the traffic volume and toll rate for different benefit functions are plotted in **Fig. 9**. The box bound of the toll rate is [$1, $20]; The structural safety constraint in this example is assumed as follows:

$$W(\boldsymbol{v}) = 3\frac{\sum_{k\in\mathcal{K}} v_k \cdot \alpha_k}{y} + 0.3 < L_{max} \tag{20}$$

Table 3: Three types of benefit functions

Type	Equation	Parameter values
(I) Negative exponential	$B(v) = (-1/b_{ne})\ln(v/q_{ne}^0)$	$b_{ne} = 0.15,\ q_{ne}^0 = 30000$
(II) Linear	$B(v) = b_l\xi_l - \eta_l v$	$b_l\xi_l = 30,\ \eta_l = 0.005$
(III) Polynomial	$B(v) = 0.015{\xi_p}^{1.05} - 0.0002v^{1.4}$	$\xi_p = 1300$

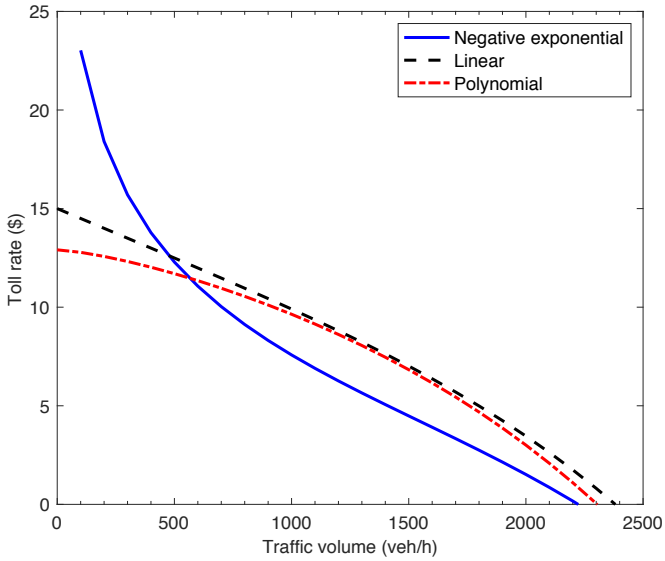

Fig. 9: The relationship between toll rate and traffic volume for three benefit functions

The optimization challenge is a traditional nonlinear optimization task; in this paper, we use the optimization toolbox in Matlab®. According to the calculation in Section 5.3, the reserve capacity of the bridge under study can be 1.30, 1.40 and 1.49 for various uncertainty assumptions. For each possible reserve capacity, the optimal operating profits and corresponding toll rates are reported in **Table 4**. Comparing to the case without reserve capacity (=1.0), , when reserve capacity is equal to 1.30, the optimal profit can be increased by 18.2%, 37.0% and 40.5% for negative exponential, linear and polynomial function respectively. The corresponding toll rates are decreased by 19.8%, 8.9% and 7.7%. When reserve capacity changes from 1.30 (the lowest estimation) to 1.49 (the largest estimation), the optimal profit increases 5%, 13.2% and 14.9% for negative exponential, linear and polynomial function respectively. The corresponding toll rates decrease by 12.4%, 6.2% and 5.6%.

Table 4: Optimal operating profit for various reserve capacities in Scenario I

Reserve capacity	Benefit function					
	(I) Negative exponential		(II) Linear		(III) Polynomial	
	Operating profit (per year) (M$)	Toll rate ($)	Operating profit (per year) (M$)	Toll rate ($)	Operating profit (per year) (M$)	Toll rate ($)
1.0	22.0	12.1	22.7	12.4	21.0	11.7
1.30	26.0	9.7	31.1	11.3	29.5	10.8
1.40	26.8	9.1	33.4	10.9	31.9	10.5
1.49	27.3	8.5	35.2	10.6	33.9	10.2

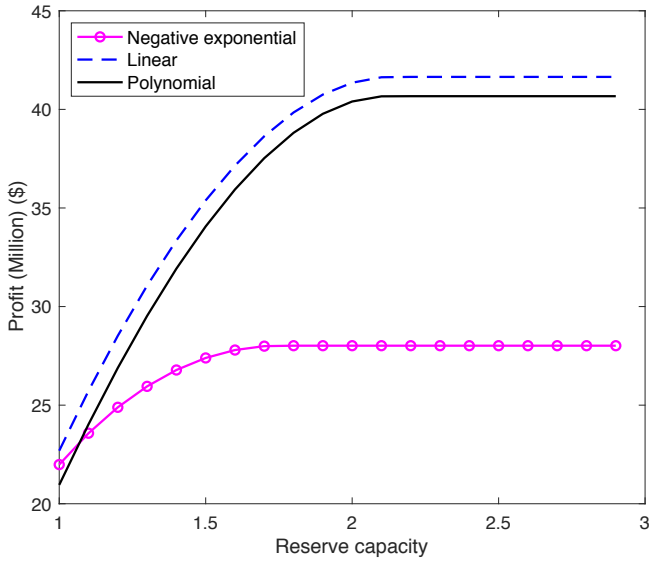

Fig. 10: Optimal operating profit over reserve capacity in Scenario I

To further investigate the influence of reserve capacity on the optimal profit, hypothetical reserve capacities ranging from 1 to 3 are studied (shown in **Fig. 10**). The linear benefit function results in the highest profit followed by the negative exponential and polynomial benefit function before the reserve capacity is larger than 1.1. After it reaches 1.1, the polynomial benefit function surpasses the negative exponential benefit function and obtains the second highest profit. The optimal operating profit peaks when the reserve capacity is 2.2 (polynomial benefit function), 2.2 (linear benefit function) and 1.8 (negative exponential benefit function). Ideally, if there is enough reserve capacity, the optimal profit is 94% (polynomial benefit function), 84% (linear benefit

function) and 27% (negative exponential benefit function) larger than the one when there is no reserve capacity.

It can be inferred from the results that for all three benefit functions, the optimal operating profit increases with the reserve capacity until the latter exceeds a certain value. When the profit reaches a peak, the corresponding reserve capacity varies according to different benefit functions. After reaching the peak, the profit remains constant and does not change further with reserve capacity. As illustrated in the previous section, the reserve capacity demonstrates the additional loads that an existing bridge can take compared with the design traffic loads. The additional loads transform into larger traffic demand (toll-dependent, see Equation (4)) when the reserve capacity is introduced in the optimization scheme, leading to a higher profit.

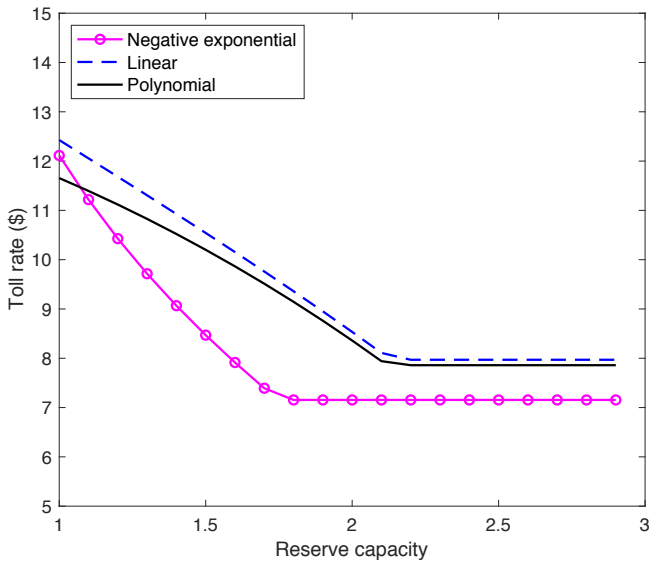

Fig. 11: Optimal operating profit over toll rate in Scenario I

The relation between the toll rate and reserve capacity is illustrated in **Fig. 11**. With the increase of reserve capacity, the toll rate decreases. The decreasing trend stops when the reserve capacity reaches a certain value. This is consistent with the performance of the optimal profit in **Fig. 10**. After the reserve capacity reaches 1.1, the

order of toll rates changes from $x_{Linear} > x_{NE} > x_{Poly}$ to $x_{Linear} > x_{Poly} > x_{NE}$. At the final stage, the toll rate decreases by 33% (polynomial benefit function), 36% (linear benefit function) and 41% (negative exponential benefit function) when compared with the one when there is no reserve capacity.

It can be inferred that by introducing reserve capacity as a safety constraint, the optimal toll rate decreases considerably which is beneficial to the highway users. With consideration of reserve capacity, the highway is able to take on larger traffic volume and heavier vehicles without compromising safety. As a result, the private firm is able to achieve optimal profit through lower prices with greater traffic volume.

5.4.2 Scenario II: Heterogeneous traffic

Vehicles on the highway can be classified into three vehicle types: passenger cars, light trucks (2 axles) and heavy trucks (5-axle semi-trailers) [47]. In this case, the travel time functions (Equation (8-10)) are adopted. The parameters of these functions are summarized in **Table 5**. The box bounds of toll rates are [$1, $40]. The structural safety constraint used in this example is assumed as follows:

$$W(\boldsymbol{v}) = 3\frac{\sum_{k\in\mathcal{K}} v_k \cdot \alpha_k}{y} + \rho_h + 0.3 \tag{21}$$

Table 5: Prespecified parameters of the travel time function and the benefit function for three types of vehicles

Parameter		Passenger car ($\boldsymbol{k}$ = 1)	Light truck ($\boldsymbol{k}$ = 2)	Heavy truck ($\boldsymbol{k}$ = 3)
Passenger car unit $\boldsymbol{\alpha_k}$		1	1.5	2.5
Value of time $\boldsymbol{\beta_k}$ ($\$/\boldsymbol{h}$) *		15	27.5	50
Free flow travel time $\boldsymbol{tt_k^0}$ (hour)		0.4	0.5	0.55
Linear benefit function	$b_l\xi_l$	30	45	60
	η_l	0.005		
Polynomial benefit function	ξ_p	1300	2300	3000

Note: * Vehicle parameters referenced from [47].

The results of the optimal profit and toll rates are shown in **Table 6**. For the lowest estimate (reserve capacity is equal to 1.30), the optimal profit increases from 43.1 M$ to 61.5 M$ under linear and from 49.1M$ to 71.2M$ polynomial functions compared with no reserve capacity. When reserve capacity is 1.49 (the highest estimation), the profit increases by 18.2% and 19.1% under linear and polynomial functions compared with the estimation of 1.30.

Table 6: Optimal operating profit for various reserve capacities in Scenario II

Reserve capacity	**Benefit function**			
	(I) Linear		(II) Polynomial	
	Operating profit (per year) (M$)	Toll rate ($)	Operating profit (per year) (M$)	toll rate ($)
1.0	43.1	x_1= 21.8	49.1	x_1= 21.2
		x_2= 30.7		x_2= 36.3
		x_3= 32.3		x_3= 39.4
1.30	61.5	x_1= 21.2	71.2	x_1= 20.9
		x_2= 30.1		x_2= 35.7
		x_3= 32.1		x_3= 39.2
1.40	67.5	x_1= 21.0	78.4	x_1= 20.8
		x_2= 30.1		x_2= 35.5
		x_3= 32.0		x_3= 39.2
1.49	72.7	x_1= 20.8	84.8	x_1= 20.6
		x_2= 29.8		x_2= 35.3
		x_3= 31.9		x_3= 39.0

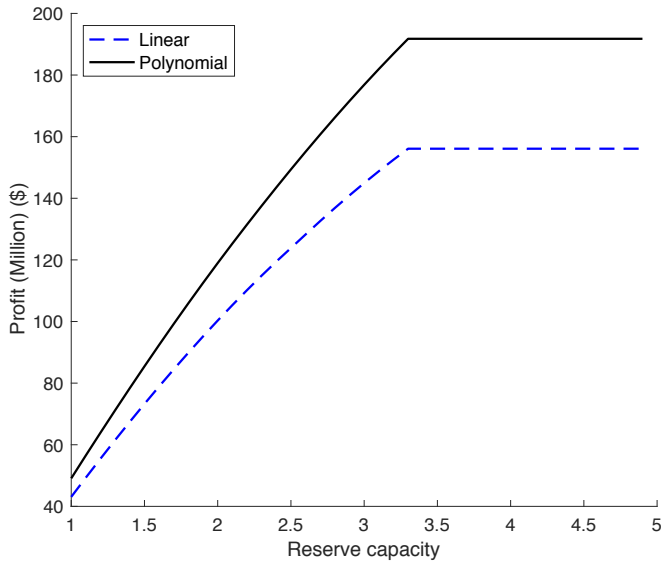

Fig. 12: Optimal operating profit over toll rate in Scenario II

For heterogeneous traffic, we investigate the optimal operating profit under reserve capacity ranging from 1 to 5. **Fig. 12** and **Fig. 13** show the projected optimal operating profits and toll rates at different levels of reserve capacity.

The same trend is observed in Scenario II. The optimal profit increases with reserve capacity until it reaches its maximum when reserve capacity is equal to 3.3 for both the polynomial benefit function and the linear benefit function. In this case study, the profit using the polynomial benefit function is always larger than the profit using the one with linear benefit function.

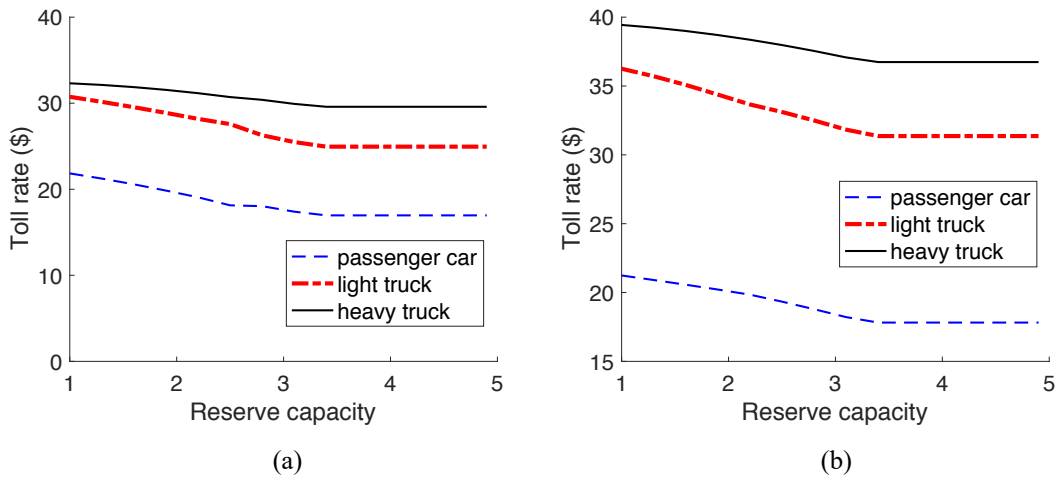

(a) (b)

Fig. 13: The relation between reserve capacity and toll rates in Scenario II: (a): linear benefit function; (b): polynomial benefit function

As shown in **Fig. 13**, for both benefit functions, the optimal toll rate of the heavy truck is always the highest, followed by the light truck and passenger car. With enough reserve capacity, the optimal toll rates are decreased by 16% (passenger car), 13% (light truck) and 7% (heavy truck) for linear benefit function, 22% (passenger car), 19% (light truck) and 8% (heavy truck) for the polynomial benefit function comparing to the case where there is no reserve capacity.

To summarize, in both Scenario I and Scenario II, the optimal operating profit increases with reserve capacity until reserve capacity reaches a certain value (as shown in **Fig. 10** and **Fig. 12**). Due to the consideration of three vehicle types, private firms manage to achieve the optimal profit not only by decreasing the toll rates (to obtain larger traffic demand) but also by increasing the ratio of heavy vehicles.

6. Discussion and limitations

In this study, we propose a framework for maximizing the operating profit of toll highways by adjusting toll rates in order to account for updated safety condition assessments of young bridges. The toll rates represent the total charge of the whole

highway. They are generally higher than the ones in reality since only private profit in the operating period is considered in this paper. For a complete design and evaluation of road pricing, the optimal BOT contract is usually a trade-off between private profit and social welfare. In this paper, three simplified benefit functions [46] are studied to demonstrate the impact of bridge capacity on highway profits. Nevertheless, in real applications, the benefit function is determined by many country/region specific factors, including the network of highways, the presence of a detour option, traffic congestion and the local economy.

For old bridges, the profit calculation will be more complicated due to the complexity of maintenance and rehabilitation. Besides, the condition assessments before and after the maintenance and rehabilitation are accordingly more complicated with special emphasis on the structural behaviour of the damaged area.

As discussed in Section 5.4, it is assumed that good estimates of extreme loading are dependent on traffic volume and heavy vehicle proportion. When such a dependency is not present through the research in the local traffic environment, the proposals in this paper are not appropriate.

7. Conclusions

This study focuses on the effects of bridge reserve capacity on the optimal operating profit of highway projects. It is motivated by two factors (i) bridges are usually subjected to critical loading constraints in highway projects, and (ii) quantitative estimates of reserve capacity can be conducted through structural system identification. The specific conclusions are as follows:

- The proposed framework allows a quantification of the impact of reserve capacity on the optimal operating profit of toll highways by adjusting toll rates

while taking into account the updated safety condition of highway bridges as a constraint of the optimization problem. In the case study, at least 18.2% additional profit could be achieved by considering the most conservative reserve capacity with the most conservative benefit function compared with the case without consideration of reserve capacity in the optimization.

- The optimal operating profit of highways increases with the reserve capacity of bridges until the loading constraint is no longer critical. This applies consistently to both homogeneous and heterogeneous traffic and for each one of the benefit functions considered (polynomial, linear and negative exponential function).
- Introducing reserve capacity as a constraint in the operating profit scheme gives an explicit interpretation of the value of structural identification and at the same time provides more flexibility to decision makers. Use of reserve capacity is promising to narrow the gap between the increasing demand and insufficient supply of infrastructure in many countries. Furthermore, the potential of improved economic returns is expected to encourage private firms to invest more in quantitative condition assessments of critical civil infrastructure.

Acknowledgment

This research was conducted at the Future Cities Laboratory at the Singapore-ETH Centre (SEC). The SEC was established as a collaboration between ETH Zurich and National Research Foundation (NRF) Singapore (FI370074016) under the auspices of the NRF's Campus for Research Excellence and Technological Enterprise (CREATE) programme. The authors would like to gratefully acknowledge the support of the Land Transport Authority of Singapore (LTA) to perform the case study. The authors wish to address that any opinions, findings, and conclusions or recommendations expressed

in this paper are those of the authors and do not reflect the views of the LTA. The authors would like to thank Prof Qiang Meng and Dr. Lu Zhaoyang for their helpful advice on BOOT projects. The authors would also like to thank Dír. Marco Proverbio for the valuable advice and support.

Reference

[1] C. M. Tam, "Build-operate-transfer model for infrastructure developments in Asia: Reasons for successes and failures," *Int. J. Proj. Manag.*, vol. 17, no. 6, pp. 377–382, Dec. 1999.

[2] J. Liu, P. E. D. Love, J. Smith, M. Regan, and P. R. Davis, "Life Cycle Critical Success Factors for Public-Private Partnership Infrastructure Projects," *J. Manag. Eng.*, 2014.

[3] "More PPP projects implemented as China seeks infrastructure funding," 2017. [Online]. Available: http://www.chinadaily.com.cn/business/2017-08/04/content_30348171.htm. [Accessed: 04-Aug-2017].

[4] H. Yang, W. Xu, B. He, and Q. Meng, "Road pricing for congestion control with unknown demand and cost functions," *Transp. Res. Part C Emerg. Technol.*, vol. 18, no. 2, pp. 157–175, 2010.

[5] G. Santos and J. Bhakar, "The impact of the London congestion charging scheme on the generalised cost of car commuters to the city of London from a value of travel time savings perspective," *Transp. Policy*, vol. 13, no. 1, pp. 22–33, Jan. 2006.

[6] L. Rotaris, R. Danielis, E. Marcucci, and J. Massiani, "The urban road pricing scheme to curb pollution in Milan, Italy: Description, impacts and preliminary cost–benefit analysis assessment," *Transp. Res. Part A Policy Pract.*, vol. 44, no. 5, pp. 359–375, Jun. 2010.

[7] M. Gibson and M. Carnovale, "The effects of road pricing on driver behavior and air pollution," *J. Urban Econ.*, vol. 89, pp. 62–73, Sep. 2015.

[8] M. A. Soomro and X. Zhang, "Roles of Private-Sector Partners in Transportation Public-Private Partnership Failures," *J. Manag. Eng.*, vol. 31,

no. 4, 2013.

[9] Q. Meng and X. Wang, “Sensitivity analysis of logit-based stochastic user equilibrium network flows with entry-exit toll schemes,” *Comput. Civ. Infrastruct. Eng.*, vol. 23, no. 2, pp. 138–156, Jan. 2008.

[10] Z. Lu and Q. Meng, “Impacts of pavement deterioration and maintenance cost on Pareto-efficient contracts for highway franchising,” *Transp. Res. Part E Logist. Transp. Rev.*, vol. 113, pp. 1–21, May 2018.

[11] X. He, X. (Michael) Chen, C. Xiong, Z. Zhu, and L. Zhang, “Optimal time-varying pricing for toll roads under multiple objectives: A simulation-based optimization approach,” *Transp. Sci.*, vol. 51, no. 2, pp. 412–426, May 2017.

[12] A. Teughels and G. De Roeck, “Structural damage identification of the highway bridge Z24 by FE model updating,” *J. Sound Vib.*, vol. 278, no. 3, pp. 589–610, 2004.

[13] J. M. W. Brownjohn, P. Moyo, P. Omenzetter, and Y. Lu, “Assessment of highway bridge upgrading by dynamic testing and finite-element model updating,” *J. Bridg. Eng.*, vol. 8, no. 3, pp. 162–172, 2003.

[14] G. Augusti, M. Ciampoli, and D. M. Frangopol, “Optimal planning of retrofitting interventions on bridges in a highway network,” *Eng. Struct.*, vol. 20, no. 11, pp. 933–939, Nov. 1998.

[15] I. F. C. Smith, “Studies of Sensor Data Interpretation for Asset Management of the Built Environment,” *Front. Built Environ.*, vol. 2, p. 8, Mar. 2016.

[16] E. Simoen, G. De Roeck, and G. Lombaert, “Dealing with uncertainty in model updating for damage assessment: A review,” *Mech. Syst. Signal Process.*, vol. 56, pp. 123–149, 2015.

[17] J. M. W. Brownjohn, A. De Stefano, Y.-L. Xu, H. Wenzel, and A. E. Aktan, “Vibration-based monitoring of civil infrastructure: challenges and successes,” *J. Civ. Struct. Heal. Monit.*, vol. 1, no. 3–4, pp. 79–95, 2011.

[18] M. Hiatt *et al.*, “Finite element model updating of a PSC box girder bridge using ambient vibration test,” *Adv. Mater. Res.*, vol. 168–170, pp. 2263–2270, Dec. 2010.

[19] N. M. Okasha, D. M. Frangopol, and A. D. Orcesi, “Automated finite element updating using strain data for the lifetime reliability assessment of bridges,” *Reliab. Eng. Syst. Saf.*, vol. 99, pp. 139–150, Mar. 2012.

[20] K. V. Yuen, *Bayesian Methods for Structural Dynamics and Civil Engineering*. 2010.

[21] Katafygiotis; J. L. Beck, “Updating models and their uncertainties. I: Bayesian statistical framework,” *J. Eng. Mech.*, vol. 124(4), no. April, pp. 463–467, 1998.

[22] S. H. Cheung and J. L. Beck, “Bayesian model updating using hybrid Monte Carlo simulation with application to structural dynamic models with many uncertain parameters,” *J. Eng. Mech.*, vol. 135, no. 4, pp. 243–255, Apr. 2009.

[23] J.-A. Goulet and I. F. C. Smith, “Structural identification with systematic errors and unknown uncertainty dependencies,” *Comput. Struct.*, vol. 128, pp. 251–258, 2013.

[24] S. G. S. Pai, A. Nussbaumer, and I. F. C. Smith, “Comparing structural identification methodologies for fatigue Life prediction of a highway bridge,” *Front. Built Environ.*, vol. 3, no. January, pp. 1–15, 2018.

[25] R. Pasquier and I. F. C. Smith, “Iterative structural identification framework for evaluation of existing structures,” *Eng. Struct.*, vol. 106, pp. 179–194, 2016.

[26] X. Guo and H. Yang, “Analysis of a build-operate-transfer scheme for road franchising,” *Int. J. Sustain. Transp.*, vol. 3, no. 5–6, pp. 312–338, Aug. 2009.

[27] T. A. Manual, “Bureau of Public Roads.” US Department of Commerce, 1964.

[28] Z. Lu, Q. Meng, and G. Gomes, “Estimating link travel time functions for heterogeneous traffic flows on freeways,” *J. Adv. Transp.*, vol. 50, no. 8, pp. 1683–1698, 2016.

[29] J.-A. Goulet, P. Kripakaran, and I. F. C. Smith, “Multimodel structural performance monitoring,” *J. Struct. Eng.*, vol. 136, no. 10, pp. 1309–1318, Oct. 2010.

[30] R. Pasquier, L. D. Angelo, J.-A. Goulet, C. Acevedo, A. Nussbaumer, and I. F. C. Smith, “Measurement, data interpretation, and uncertainty propagation for

fatigue assessments of structures," *J. Bridg. Eng.*, vol. 21, no. 5, p. 4015087, 2016.

[31] R. Pasquier, J.-A. Goulet, C. Acevedo, and I. F. C. Smith, "Improving fatigue evaluations of structures using in-service behavior measurement data," *J. Bridg. Eng.*, vol. 19, no. 11, p. 04014045, 2014.

[32] M. Proverbio, D. G. Vernay, and I. F. C. Smith, "Population-based structural identification for reserve-capacity assessment of existing bridges," *J. Civ. Struct. Heal. Monit.*, vol. 8, no. 3, pp. 363–382, 2018.

[33] EN 1990, "Eurocode - Basis of structural design," *CEN, European Committee for Standardization*. 2005.

[34] *fib Model Code for Concrete Structures*. 2010.

[35] S.-H. Kim, W.-H. Heo, D. You, and J.-G. Choi, "Vehicle loads for assessing the required load capacity considering the traffic environment," *Appl. Sci.*, vol. 7, no. 4, p. 365, Apr. 2017.

[36] C. Leahy, E. OBrien, and A. O'Connor, "The Effect of Traffic Growth on Characteristic Bridge Load Effects," *Transp. Res. Procedia*, vol. 14, pp. 3990–3999, 2016.

[37] E. J. OBrien, A. Bordallo-Ruiz, and B. Enright, "Lifetime maximum load effects on short-span bridges subject to growing traffic volumes," *Struct. Saf.*, vol. 50, pp. 113–122, 2014.

[38] Y. Yu, C. S. Cai, W. He, and H. Peng, "Prediction of bridge maximum load effects under growing traffic using non-stationary bayesian method," *Eng. Struct.*, vol. 185, no. July 2018, pp. 171–183, 2019.

[39] W.-J. Cao, C. G. Koh, and I. F. C. Smith, "Enhancing static-load-test identification of bridges using dynamic data," *Eng. Struct.*, vol. 186, pp. 410–420, 2019.

[40] C. E. Rasmussen and C. K. I. Williams, *Gaussian processes for machine learning.* the MIT Press, 2006.

[41] B. Enright, E. J. OBrien, and C. Leahy, "Identifying and modelling permit trucks for bridge loading," *Proc. Inst. Civ. Eng. - Bridg. Eng.*, vol. 169, no. 4,

pp. 235–244, 2016.

[42] Eurocode, *EN 1992 -Design of concrete structures*. 2004.

[43] T. Lai, T. H. Yi, and H. N. Li, "Parametric study on sequential deconvolution for force identification," *J. Sound Vib.*, vol. 377, pp. 76–89, 2016.

[44] H. Schlune, M. Plos, and K. Gylltoft, "Safety formats for non-linear analysis of concrete structures," *Mag. Concr. Res.*, vol. 64, no. 7, pp. 563–574, 2012.

[45] M. Fernández Ruiz and A. Muttoni, "On development of suitable stress fields methods for structural concrete," *ACI Struct. J.*, no. 104, pp. 495–502, 2008.

[46] Z. Lu, "Analysis of design factors for highway franchising (doctoral dissertation)," National University of Singapore, 2016.

[47] J. Holguín-Veras and M. Cetin, "Optimal tolls for multi-class traffic: Analytical formulations and policy implications," *Transp. Res. Part A Policy Pract.*, vol. 43, no. 4, pp. 445–467, 2009.